

Article

## Generation of Free $\text{OH}_{\text{aq}}$ Radicals by Black Light Illumination of Degussa (Evonik) P25 $\text{TiO}_2$ Aqueous Suspensions

Haidong Liao <sup>1,\*</sup> and Torbjörn Reitberger <sup>2</sup>

<sup>1</sup> Wallenius Water AB, Franzéngatan 3, SE-112 51 Stockholm, Sweden

<sup>2</sup> KTH Chemical Science and Engineering, Applied Physical Chemistry, Royal Institute of Technology, SE-100 44 Stockholm, Sweden; E-Mail: torbreit@kth.se

\* Author to whom correspondence should be addressed; E-Mail: haidong.liao@walleniuswater.com; Tel.: +46-812-013-844; Fax: +46-852-272-299.

Received: 16 December 2012; in revised form: 23 January 2013 / Accepted: 22 March 2013 / Published: 16 April 2013

---

**Abstract:** This work demonstrates how formation of strongly chemiluminescent 3-hydroxyphthalic hydrazide by hydroxylation of non-chemiluminescent phthalic hydrazide can be applied as a selective reaction probe to obtain information on authentic hydroxyl radical, *i.e.*,  $\cdot\text{OH}_{\text{aq}}$ , formation, in black light illuminated Degussa P25  $\text{TiO}_2$  aerated suspensions in the pH range from 3 to 11. The  $\cdot\text{OH}_{\text{aq}}$  formation was found to be strongly pH dependent. At alkaline pH, the apparent quantum efficiency of  $\cdot\text{OH}_{\text{aq}}$  formation was estimated to be at the  $\sim 10^{-2}$  level whereas at acidic pH it was near zero. Addition of phosphate and fluoride ions substantially enhanced the  $\cdot\text{OH}_{\text{aq}}$  production in the acidic pH range. It is suggested that  $\cdot\text{OH}_{\text{aq}}$ -radical formation in  $\text{TiO}_2$  photocatalysis can occur by oxidation of hydroxyl ions in the water layer adsorbed on  $\text{TiO}_2$  surfaces.

**Keywords:** photocatalysis;  $\text{TiO}_2$ ;  $\cdot\text{OH}_{\text{aq}}$  radical; chemiluminescence

---

### 1. Introduction

In semiconductor materials, absorption of photons with energy greater than the band gap between the valence and conduction bands leads to the formation of valence band holes ( $h_{\text{VB}}^+$ ) and conduction band electrons ( $e_{\text{CB}}^-$ ). Usually, an electron-hole pair has only transient existence and is rapidly eliminated by recombination resulting in heat or light emission, but in some large band gap materials the lifetime is long enough to allow a fraction of hole-electron pairs to be manifested on the material

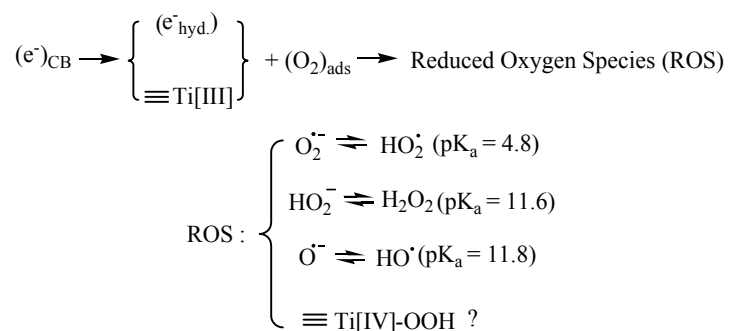
surface by inducing red-ox reactions in the surrounding medium. Materials displaying these characteristics are called photocatalysts [1]. Amongst different materials showing photocatalytic properties, Titania,  $\text{TiO}_2$ , has been identified as the most interesting due to its otherwise inert and environmentally friendly properties. In the last two decades, photocatalysis utilizing  $\text{TiO}_2$  has been gaining increasing popularity as an attractive advanced oxidation technique for treatment of industrial, potable and natural waters by removing chemical and microbiological hazards without addition of (toxic) chemicals [2–6].

Titania exists in three crystalline polymorphs; anatase, rutile and brookite. Of these, only anatase and rutile show substantial photocatalytic activity. Many studies have confirmed that anatase presents better photocatalytic properties than rutile due to a lower intrinsic recombination rate of photogenerated hole-electron pairs. However, mixed phase titania such as Degussa P25 containing nanoclusters of rutile in anatase crystallites shows even better photo activity than pure phase anatase and has been used in most photocatalytic studies [7]. The material is also easily available and was chosen for this study.

Anatase  $\text{TiO}_2$  has a band gap of  $\sim 3.2$  eV with the valence band edge  $+2.6$  V vs. NHE, and the conduction band edge  $-0.6$  V vs. NHE at pH 7 [8,9]. Thus, absorption of photons at wavelengths  $< 390$  nm in this material leads to the generation of electron hole pairs. Following this initial step, conduction band electrons ( $e_{\text{CB}}^-$ ) and valence band holes ( $h_{\text{VB}}^+$ ) must be trapped at the surface to allow chemical transformations in the surrounding medium.

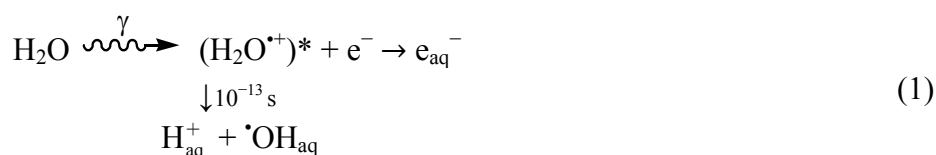
The trapping of conduction band electrons ( $e_{\text{CB}}^-$ ) may chemically be associated with formation of  $\equiv\text{Ti}[\text{III}]^*$ -centers and/or partially hydrated electrons ( $e_{\text{hyd}}^-$ ) on the particle surface [10,11]. In air saturated aqueous solutions, it is likely that oxygen adsorbed on  $\text{TiO}_2$  surfaces will react with partially hydrated electrons ( $e_{\text{hyd}}^-$ ) and  $\equiv\text{Ti}[\text{III}]^*$ -centers on the surface by initial formation of reduced oxygen species (ROS), Figure 1.

**Figure 1.** Reduction of adsorbed oxygen and formation of ROS (pKa-values [12]). When the  $\text{TiO}_2$  surface is coated in places with nano-dots of a noble metal such as Pt, conduction band electrons ( $e_{\text{CB}}^-$ ) can be directly trapped by Pt nano-particles on a  $\text{TiO}_2$  surface, *i.e.*,  $(e_{\text{CB}}^-) + \text{Pt} \rightarrow (e_{\text{Pt}}^-)$  [13].  $(e_{\text{Pt}}^-)$  may be more reducing than  $(e_{\text{hyd}}^-)$  (*vide infra*). Formation of hydroperoxides in  $\text{TiO}_2$  photocatalysis was shown by Nakamura *et al.* [14] using multiple internal reflection infrared microscopy. Hydroxyl radicals are probably formed by catalyzed cleavage of hydrogen peroxide.



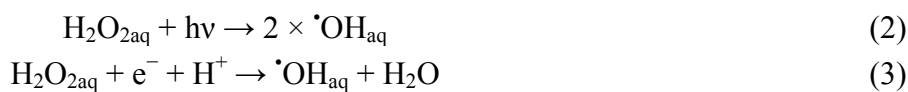
Depending on the reaction environment, pH and ion composition, radicals and hydrogen peroxide may be preferentially bound to the surface or released to the surrounding aqueous solution.

It is reasonable to assume that valence band holes ( $h_{VB}^+$ ) reaching the  $TiO_2$  surface can be chemically associated with oxygen-centered radicals generated from surface hydroxyls [7,15], and lattice oxygen anions [10]. The specific nature of these initially formed oxygen centered surface radicals will depend on pH. Based on chemical reactivity, they are usually described as surface bound hydroxyl radicals,  $\cdot OH_{surface}$ . However, this designation is problematic as it leads the mind to consider  $\cdot OH_{surface}$  as an authentic hydroxyl radical trapped on the  $TiO_2$  surface. This is not correct. In this context it is important to note that diffusion of free hydroxyl radicals from UV-irradiated water saturated  $TiO_2$ -surfaces to the gas phase has been shown by laser-induced excitation spectroscopy [16]. Thus, direct physical evidence strongly supports that UV-irradiation of  $TiO_2$  can in fact also release free hydroxyl radicals to the surrounding medium, *i.e.*, formation of  $\cdot OH_{aq}$ . Since  $\cdot OH_{aq}$  reacts exceedingly fast with most solutes it will only diffuse a very short distance from the surface, typically <50 nm, before it is consumed. For this reason, it may seem unimportant to discriminate between  $\cdot OH_{surface}$  and  $\cdot OH_{aq}$ . However, only the latter can be expected to behave completely as authentic free hydroxyl radicals generated by, e.g., radiolysis of water [12]:



where  $(H_2O^{+\bullet})^*$  denotes an excited state due to a Frank-Condon transition

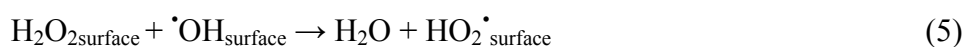
There is still a controversy about whether valence band holes ( $h_{VB}^+$ ), are involved in the formation of  $\cdot OH_{aq}$  radicals in  $TiO_2$  photocatalysis [17–21]. Formation of  $\cdot OH_{aq}$  can also proceed by homolytic and/or reductive cleavage of accumulated hydrogen peroxide formed by oxygen reduction initiated by conduction band electrons ( $e_{CB}^-$ ), *cf.* Figure 1. In fact, most investigators seem to prefer this reaction model.



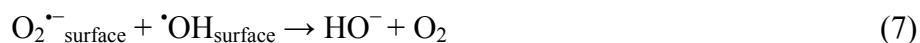
Reaction (2) is efficient in the UVC (200~280 nm) range, where the absorption by hydrogen peroxide is significant [22]. Reaction (3) may occur by way of surface excess electrons, e.g., trapped on Pt nano-particles:



Accumulation of reduced oxygen species on the  $TiO_2$  surface may also cause back-reactions that impair the formation of hydroxyl radicals, e.g.,



and perhaps most importantly:



(O<sub>2</sub> formed in Reactions (6) and (7) may be singlet excited and chemically reactive).

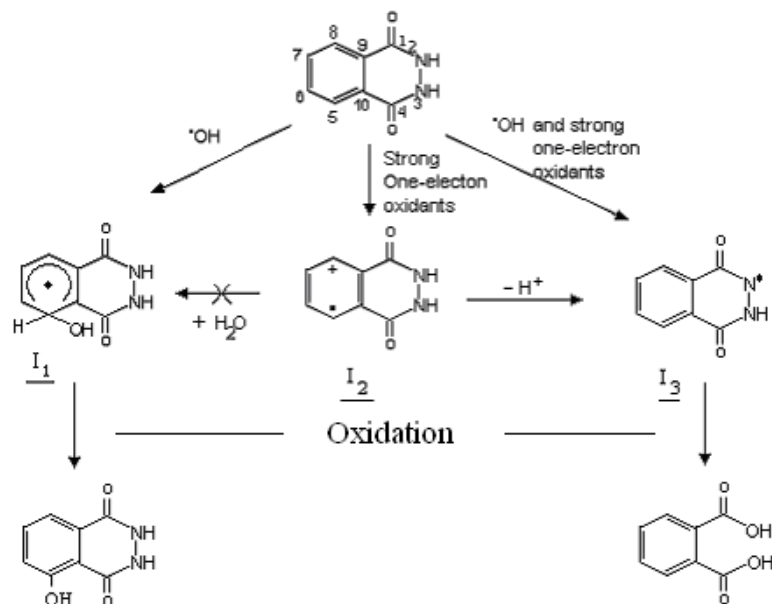
These back reactions can be considered as delayed recombinations of valence band holes (h<sub>VB</sub><sup>+</sup>) and conduction band electrons (e<sub>CB</sub><sup>-</sup>). As both direct and delayed recombinations of hole-electron pairs follow second order kinetics, they will gain in importance with increasing light intensity.

The formation of hydroxyl radicals in TiO<sub>2</sub> photocatalysis has also been studied with various chemical reaction probes, e.g., formation of formaldehyde by oxidation of methanol [23] or TRIS [24], hydroxylation of aromatic compounds [19,25,26], and formation of hydroxyl radical spin-trap adducts [27]. However, these reaction probes can generally not discriminate between reactions involving <sup>•</sup>OH<sub>surface</sub> and <sup>•</sup>OH<sub>aq</sub> radicals. Moreover, one-electron oxidation and hydration of the intermediate radical cation, e.g., formed by a direct hole (h<sub>VB</sub><sup>+</sup>) induced oxidation on the TiO<sub>2</sub> surface, can give the same reaction product as with authentic hydroxyl radicals. Evidently, adsorption of the reaction probe can profoundly alter the result of measurement.

The present investigation is an attempt to investigate the formation of <sup>•</sup>OH<sub>aq</sub> radicals in TiO<sub>2</sub> photocatalysis using a selective chemical reaction probe based on hydroxylation of non-chemiluminescent phthalic hydrazide (concentration ≤ 0.5 mM) to give the strongly chemiluminescent 3-hydroxyphthalic hydrazide (iso-electronic to luminol). At selected time intervals, a small sample aliquot of the reaction liquor is transferred to a luminometer where chemiluminescence is developed by oxidation of the accumulated 3-hydroxyphthalic hydrazide to the corresponding phthalic acid [28,29]. Using this method it was possible to follow the formation and reactions of hydroxyl radicals during oxygen and hydrogen peroxide bleaching of paper pulp [28,30] as well as in metabolic processes associated with fungal growth in wood shavings [31,32], and in natural systems [33].

Possible reaction pathways during photocatalytic oxidation of phthalic hydrazide are shown in Figure 2. The phthalic hydrazide radical cation has an estimated oxidation potential of about 1.5 V vs. NHE [29], so the positive hole formed in TiO<sub>2</sub> photocatalysis can in all probability oxidize adsorbed phthalic hydrazide to its radical cation. However, since the radical cation is a strong acid (est. pK<sub>a</sub> ≤ -3 [29]) a proton is immediately eliminated from the hydrazide moiety leaving an N-centered radical that eventually results in formation of phthalic acid. Thus, the back door for formation of chemiluminescent 3-hydroxyphthalic hydrazide by addition of water to the radical cation is closed. In fact, strong chemiluminescence was only obtained when authentic hydroxyl radicals were generated by γ-irradiation, whereas no chemiluminescence could be detected when phthalic hydrazide reacted with strong one-electron oxidants such as Ce<sup>4+</sup>, Co<sup>3+</sup>, N<sub>3</sub><sup>•</sup>, HO<sub>2</sub><sup>•</sup>, CO<sub>3</sub><sup>•-</sup>, Br<sub>2</sub><sup>•-</sup> or SO<sub>4</sub><sup>•-</sup> [29]. The selectivity for the hydroxyl radical also excludes the oxyl radical anion, O<sup>•-</sup>, since virtually no chemiluminescence was observed at pH > 12. (pK<sub>a</sub> of HO<sup>•</sup> = 11.9 [12]).

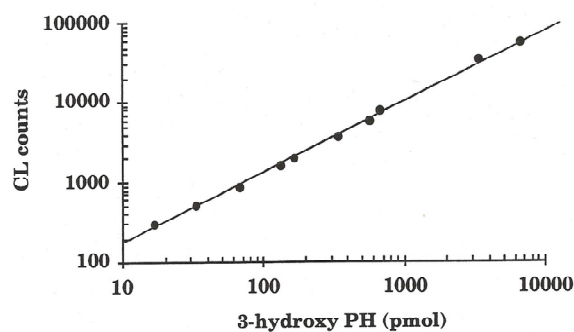
**Figure 2.** Reactions occurring when phthalic hydrazide reacts with hydroxyl radicals or strong one-electron oxidants. About 50% of hydroxyl radicals react by addition to the aromatic ring, the remainder attacks the hydrazide moiety [29]. Oxidation of I<sub>1</sub> and I<sub>3</sub> occurs spontaneously by dissolved oxygen in the reaction system.



This pH restriction also bears on other chemical reaction probes based on hydroxylation of aromatic compounds since only  $\cdot\text{OH}_{\text{aq}}$  radicals can amalgamate with  $\pi$ -electrons in an aromatic ring to form cyclohexadienyl adducts that after oxidation result in aromatic ring hydroxylation. What is generally not considered is that this oxidation is rather slow with molecular oxygen due to the reversible addition of oxygen to a hydroxycyclohexadienyl adduct [34]. At  $\text{pH} > 6$  the self-termination of superoxide is entirely proton controlled so the concentration of superoxide may become significant in alkaline solution [35]. The reaction with oxygen may then be challenged by superoxide at high pH as its reaction with a hydroxycyclohexadienyl adduct should be non-reversible and the reaction rate close to diffusion controlled (*cf.* reaction of superoxide with phenoxy-type radicals [36]). If so, a range of alternative reaction pathways are possible and the yield of aromatic ring hydroxylation could be much reduced. To summarize, the use of chemical reaction probes based on hydroxylation of aromatic compounds must be well researched at high pH to allow reliable conclusions.

In strongly acidic solution,  $\text{pH} < 3$ , the reaction  $\text{I}_1 + \text{H}^+ \rightarrow \text{H}_2\text{O} + \text{I}_2 \rightarrow \text{H}^+ + \text{I}_3$  becomes important. The recommended pH range for  $\cdot\text{OH}_{\text{aq}}$  radical detection by the phthalic hydrazide method thus lies between 3 and 11. As demonstrated by  $\gamma$ -radiolysis of phthalic hydrazide solutions [28], the chemiluminescence response is linear with the  $\cdot\text{OH}_{\text{aq}}$  radical production (up to about 20% of conversion of the initial phthalic hydrazide concentration). Also when chemiluminescence was measured *vs.* the amount of authentic 3-hydroxyphthalic hydrazide (10 pmol–10 nmol) a linear response was obtained, Figure 3.

**Figure 3.** Chemiluminescence response vs. the amount of authentic 3-hydroxyphthalic hydrazide (2,3-dihydro-1,4-phthalazinedione) synthesized according to Drew and Pearman [37]. Mean values of five measurements with a standard deviation <5% are presented in the figure.



Similarly, a linear chemiluminescence response and  $\lambda_{\max}$  at  $\sim 440$  nm is reported for solutions containing 3-hydroxyphthalic hydrazide (0–50  $\mu\text{M}$ ) [38].

Moreover, since the hydrazide moiety of the phthalic hydrazide molecule can be linked to hydroxyl groups on the  $\text{TiO}_2$  surface by strong hydrogen bonds it is likely that any surface bound oxidant will only cause oxidation according to the right side pathway in Figure 2. For this reason, chemiluminescence may only be observed if  $\cdot\text{OH}_{\text{aq}}$  radicals are formed in  $\text{TiO}_2$  photocatalysis.

In this study, we have investigated the generation of  $\cdot\text{OH}_{\text{aq}}$  radicals by black light illumination (345–385 nm) of Degussa P25  $\text{TiO}_2$  aqueous suspensions in the pH-range 3–11 by the selective phthalic hydrazide chemiluminescence method. The sensitivity of the method is extremely high allowing accurate measurements at very small radiation doses. This prevents accumulation of hydrogen peroxide which is an efficient hydroxyl radical precursor in  $\text{TiO}_2$ -photocatalysis [22]. The lower energy by the black light also reduces possible complications due to photo-ionization and photo-induced secondary reactions.

## 2. Results and Discussion

### 2.1. Gamma Radiolysis

The initial interaction of high energy  $\gamma$ -radiation with molecules in a mixture follows from their electron fractions [12]. In dilute aqueous solutions it can thus be safely assumed that all energy is absorbed by water molecules (55 M) and not by solutes (<0.1 M). As shown by Equation (1), this energy allows generation of  $\cdot\text{OH}_{\text{aq}}$  radicals by direct water oxidation, *i.e.*, without loading the reaction system with additives as required by other methods to produce hydroxyl radicals, e.g., Fenton chemistry, peroxyxynitrite, photolytic cleavage of hydrogen peroxide. Knowing the radiation dose by dosimetry, quantitative calibration of radical yields can be obtained. In fact, a  $\gamma$ -irradiation source can be considered as a radical titration apparatus, e.g., for  $\cdot\text{OH}_{\text{aq}}$ .

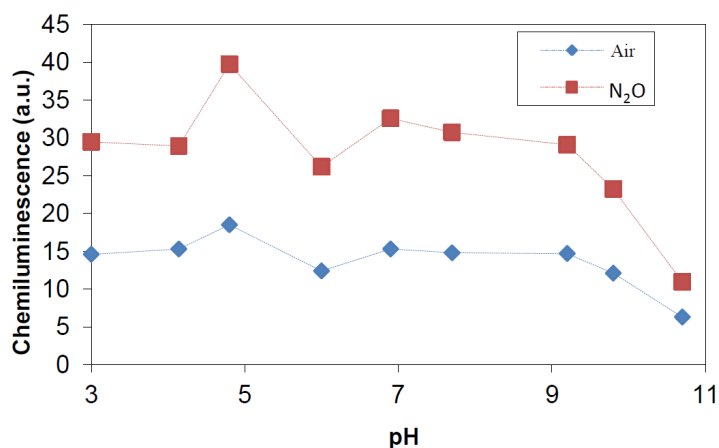
In this study, all irradiations were performed in the same vessel containing 40 mL solution. The  $\gamma$ -dose rate in this volume was determined by Fricke dosimetry [12] to be 9.5 Gy/min. This translates to a radiolytic  $\cdot\text{OH}_{\text{aq}}$  production rate of 2.70  $\mu\text{M}/\text{min}$  [12].

When dilute aqueous solutions are exposed to  $\gamma$ -irradiation, hydroxyl radicals ( $\cdot\text{OH}_{\text{aq}}$ ) and solvated electrons ( $e_{\text{aq}}^-$ ) are produced with identical yields [12], *cf.* Equation (1). In air saturated solutions, solvated electrons are rapidly scavenged by dissolved oxygen to give superoxide  $\text{O}_2^{\cdot-}$ . If solutions contain dinitrous oxide,  $\text{N}_2\text{O}$ , formation of superoxide is substituted by additional formation of hydroxyl radicals [12]:



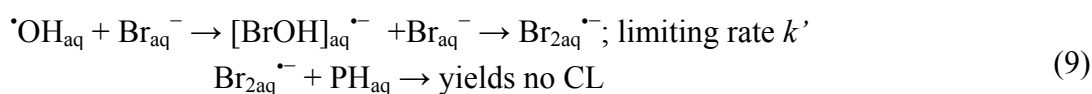
In the experiments with  $\text{N}_2\text{O}$  present, phthalic hydrazide solutions were saturated with a  $\text{N}_2\text{O}/\text{O}_2$  mixture (20%  $\text{O}_2$ ) before the irradiation. Due to a much higher solubility of  $\text{N}_2\text{O}$  over  $\text{O}_2$  (The Henry constant for  $\text{O}_2$  is  $1.3 \times 10^{-3}$  M/atm, and for  $\text{N}_2\text{O}$  is  $2.5 \times 10^{-2}$  M/atm [39]), practically all solvated electrons are scavenged by  $\text{N}_2\text{O}$  in this case. Comparisons of the chemiluminescence yields by gamma-irradiation of solutions saturated with air and with a gas mixture containing  $\text{N}_2\text{O}$  and  $\text{O}_2$  should reflect the conversion of  $e_{\text{aq}}^-$  to  $\cdot\text{OH}_{\text{aq}}$  according to reaction (8), Figure 4.

**Figure 4.** Chemiluminescence (CL) intensity (a.u.) determined at different pH by  $\gamma$ -irradiation of 0.5 mM phthalic hydrazide solutions saturated with air and with a gas mixture of 20%  $\text{O}_2$  in  $\text{N}_2\text{O}$ .

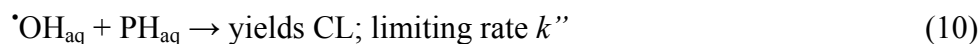


As can be seen in Figure 5, saturation with the  $\text{N}_2\text{O}/\text{O}_2$  gas mixture results in a 2.0 times stronger signal in the pH-range 3–11 as expected by Reactions (1) and (8). Another conclusion from this study is that substitution of superoxide with an additional formation of hydroxyl radicals through Reaction (8) caused no superoxide related effect, *i.e.*, in the investigated pH-range superoxide is unimportant in the chemistry of phthalic hydrazide hydroxylation.

In presence of  $\text{Br}^-$  ions hydroxyl radicals will be scavenged by formation of bromidyl radicals,  $\text{Br}_2^{\cdot-}$ : one-electron reduction potential 1.66 V [40]. Since these only oxidize the hydrazide moiety, *cf.* Figure 2, the chemiluminescence yield will be reduced by competition between the reactions:



and



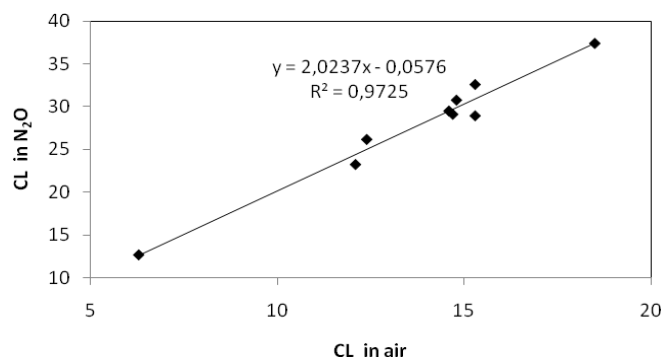
(PH: phthalic hydrazide; CL: chemiluminescence yield measured in the luminometer).

This reaction scheme translates to the equation:

$$\frac{1}{CL} = \frac{1}{CL_0} \left\{ 1 + \frac{k'[\text{Br}^-]}{k''[\text{PH}]} \right\} \quad (11)$$

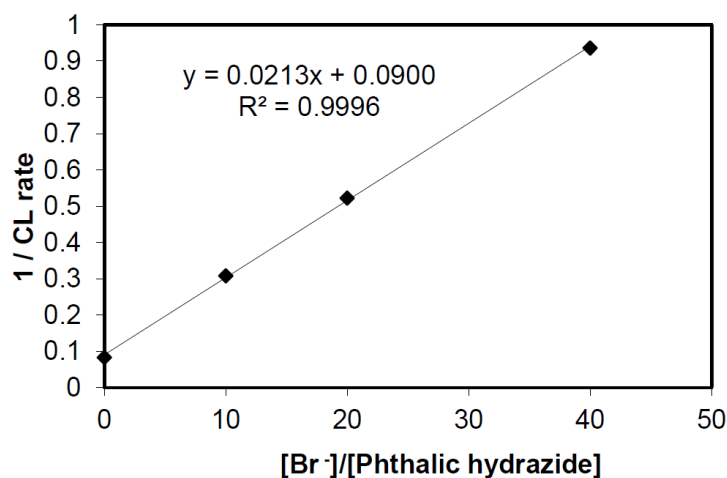
where  $CL_0$  is the chemiluminescence yield in absence of  $\text{Br}^-$ .

**Figure 5.** Data from Figure 3 plotted as CL intensity obtained with a gas mixture of 20%  $\text{O}_2$  in  $\text{N}_2\text{O}$  vs. the CL intensity obtained with air saturation at corresponding pH-values.



An experimental verification of equation 11 is shown in Figure 6 below:

**Figure 6.** Competition plot of  $1/CL$  vs.  $[\text{Br}^-]/[\text{PH}]$  in borate buffer at pH = 10.



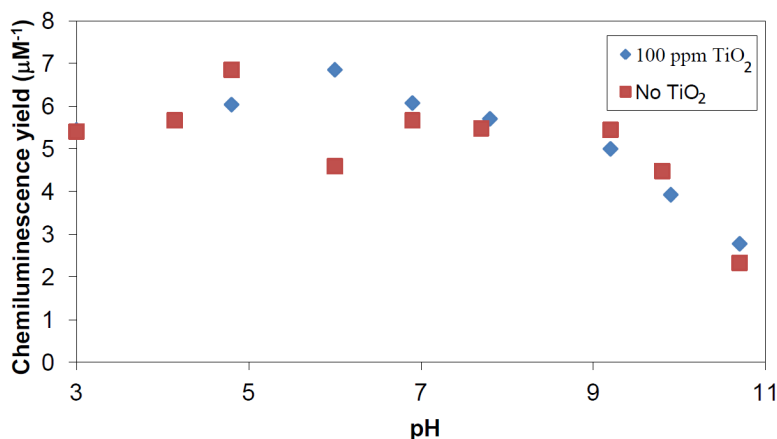
From the plot in Figure 6, we obtain  $k'/k'' = 0.0213/0.09 = 0.237$ . Since  $k'$  is reported to be  $8.0 \times 10^8/\text{M}\cdot\text{s}$  at pH 10 [41], we obtain  $k'' = 3.4 \times 10^9/\text{M}\cdot\text{s}$ . This is in excellent agreement with previously determined values which range between  $(3 \pm 1) \times 10^9/\text{M}\cdot\text{s}$  [29,42]. This demonstrates that the simple competition kinetics described in Reactions (9) and (10) is valid for authentic hydroxyl radicals, *i.e.*,  $\cdot\text{OH}_{\text{aq}}$ . Later in the discussion, Section 2.2.3, we will come back to the same experiment repeated with hydroxyl radicals generated by photocatalysis.

Lawless *et al.* [21] performed a pulse radiolysis study on colloidal 13 nm  $\text{TiO}_2$  particles at pH about 3 and reported a diffusion-controlled rate constant for the reaction of the  $\cdot\text{OH}_{\text{aq}}$  radical with these particles. This report prompted us to investigate the influence of Degussa P25  $\text{TiO}_2$  powder suspensions on the formation of chemiluminescence in the pH range 3–11 by comparing the

chemiluminescence obtained by  $\gamma$  irradiation of 0.5 mM phthalic hydrazide solutions with and without addition of 100 ppm  $\text{TiO}_2$ .

Results presented in Figure 7 show, apart from a possible irregularity at pH 6, no noticeable effects under the experimental conditions. This demonstrates that free hydroxyl radicals being generated in the reaction liquor by  $\gamma$  irradiation are not scavenged by 100 ppm P25  $\text{TiO}_2$ -particles to any significant degree in competition with 0.5 mM phthalic hydrazide. Moreover, there is no indication of a selective adsorption of formed 3-hydroxyphthalic hydrazide on  $\text{TiO}_2$  particles.

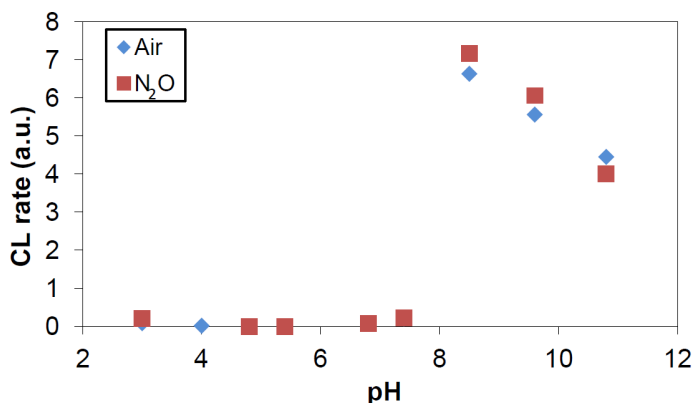
**Figure 7.** CL intensity obtained by  $\gamma$  irradiation of 0.5 mM phthalic hydrazide solutions with and without addition of 100 ppm  $\text{TiO}_2$ .



## 2.2. Photocatalysis

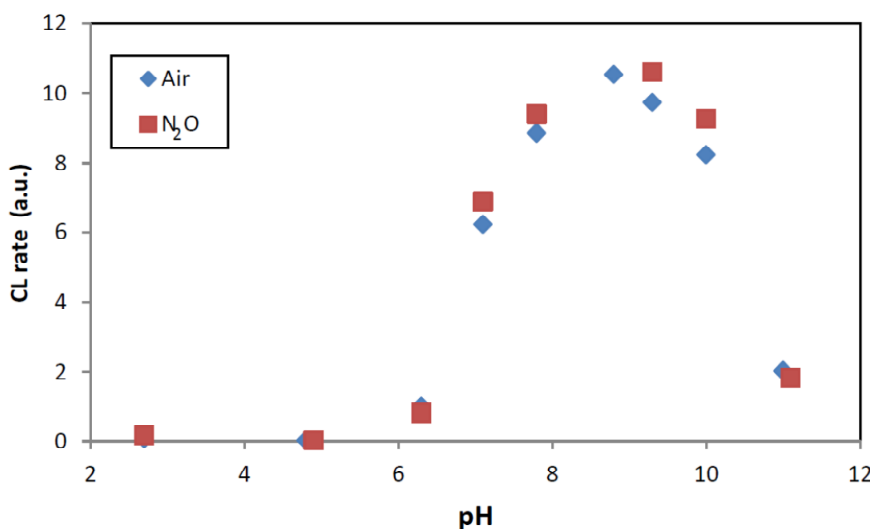
As is clearly seen in Figure 8, the chemiluminescence obtained by photo-irradiation of  $\text{TiO}_2$ -suspensions containing 100 ppm  $\text{TiO}_2$  and 0.5 mM phthalic hydrazide shows a vastly different pH-behavior from that obtained by  $\gamma$  irradiation of the same reaction system, see Figure 7. Only at  $\text{pH} > 7$  there is a significant chemiluminescence yield which at  $\text{pH} > 8.5$  follows the trend seen in Figure 7.

**Figure 8.** CL intensity as function of pH obtained by black-light irradiation of  $\text{TiO}_2$ -suspensions containing 100 ppm  $\text{TiO}_2$  and 0.5 mM phthalic hydrazide solutions saturated with air or with a gas mixture of 20%  $\text{O}_2$  in  $\text{N}_2\text{O}$ . pH was adjusted only by addition of  $\text{NaOH}$  or  $\text{HClO}_4$ .



As can be seen in Figure 9, addition of 5 mM borate buffer can profoundly increase the chemiluminescence signal at pH > 6. This demonstrates that presence of buffer can affect the measurement. This aspect is further discussed in Section 2.2.4.

**Figure 9.** CL intensity as function of pH obtained by black-light irradiation of TiO<sub>2</sub>-suspensions containing 100 ppm TiO<sub>2</sub> and 0.5 mM phthalic hydrazide solutions saturated with air or with a gas mixture of 20% O<sub>2</sub> in N<sub>2</sub>O. pH was adjusted by addition of 5 mM borate buffer and NaOH or HClO<sub>4</sub>.



It was shown by Jaesang Lee *et al.* [13] that partially hydrated electrons available on platinized TiO<sub>2</sub> are reducing enough to allow reductive cleavage of N<sub>2</sub>O, *i.e.*, by analogy with Reaction (8):

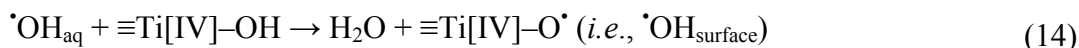


Apparently Figures 8 and 9 show no effect of N<sub>2</sub>O in photo-irradiation of TiO<sub>2</sub>-suspensions. This observation lends support to the suggestion, caption Figure 1, that (e<sub>Pt</sub><sup>-</sup>)<sub>aq</sub> is significantly more reducing than (e<sub>hyd.</sub><sup>-</sup>). In non-platinized Degussa P25, conduction band electrons trapped at the surface may be chemically associated with (e<sub>hyd.</sub><sup>-</sup>) and ≡Ti[III]<sup>•</sup>-centers. Exposing the latter to N<sub>2</sub>O may result in formation of ≡Ti[IV]-O<sup>•</sup> sites, *cf.* Shultz *et al.* [43]:



Since the concentration of N<sub>2</sub>O is much higher than that of O<sub>2</sub> in solutions saturated with a gas mixture of 20% O<sub>2</sub> in N<sub>2</sub>O (The Henry constant for O<sub>2</sub> is 1.3 × 10<sup>-3</sup> M/atm, and for N<sub>2</sub>O is 2.5 × 10<sup>-2</sup> M/atm [39]), Reaction (13) would compete successfully with formation of reduced oxygen species, Figure 1. Hence, the lack of an N<sub>2</sub>O effect also implies that ≡Ti[IV]-O<sup>•</sup> sites cannot act as precursors of <sup>•</sup>OH<sub>aq</sub>.

This conclusion bears on the results reported by Lawless *et al.* [21]. They studied acidic aqueous solutions (pH ~3) containing colloidal 13 nm TiO<sub>2</sub> particles by pulse radiolysis and reported a diffusion-controlled rate constant for the trapping of <sup>•</sup>OH<sub>aq</sub> radicals by these particles. The resulting surface bound oxidant was described as a surface trapped hydroxyl radical, <sup>•</sup>OH<sub>surface</sub>. Since colloidal TiO<sub>2</sub> particles prepared by hydrolysis of, e.g., Ti[IV]Cl<sub>4</sub>, should contain a large fraction of ≡Ti[IV]-OH sites on the surface these would react with <sup>•</sup>OH<sub>aq</sub> by:



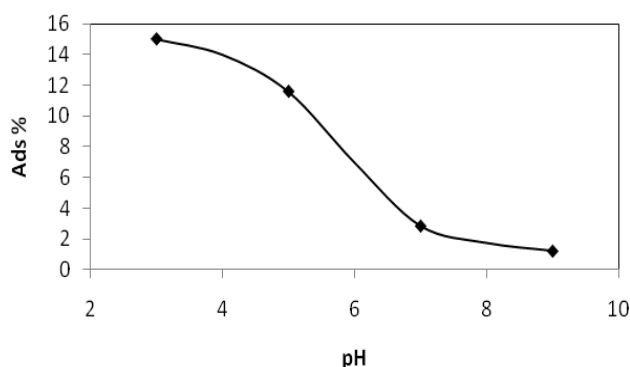
The reduction potential of  $\cdot\text{OH}_{\text{surface}}$  was assessed to be in the range 1.5–1.7 V vs. NHE. This is significantly lower than the reduction potential of the  $\cdot\text{OH}/\text{OH}$  pair at about 1.9 V [40]. Hence, thermodynamics would exclude that surface trapped hydroxyl radicals ( $\equiv\text{Ti}[\text{IV}]\text{-O}\cdot$  sites), are precursors of  $\cdot\text{OH}_{\text{aq}}$ , i.e., Reaction (14) is not reversible at any pH.

### 2.2.1. Adsorption of Phthalic Hydrazide to $\text{TiO}_2$

The chemiluminescence observed may be controlled by the amount of phthalic hydrazide being adsorbed on the  $\text{TiO}_2$  particle surfaces.

The adsorption of phthalic hydrazide to  $\text{TiO}_2$  at different pH values was checked by measuring the spectral absorption difference at 310 nm in 500  $\mu\text{M}$  phthalic hydrazide solutions before and after the addition of 100 ppm  $\text{TiO}_2$ . Suspensions containing  $\text{TiO}_2$  were filtered through a 0.2  $\mu\text{m}$  membrane filter before measurement. Results are shown below, Figure 10.

**Figure 10.** Adsorption of phthalic hydrazide to  $\text{TiO}_2$  vs. pH measured as the absorption difference at 310 nm in 500  $\mu\text{M}$  phthalic hydrazide solutions before and after the addition of 100 ppm  $\text{TiO}_2$ . When required, pH was adjusted by addition of NaOH or  $\text{HClO}_4$ .



The absorption of phthalic hydrazide at pH 3 corresponds to a density of adsorbed phthalic hydrazide on the  $\text{TiO}_2$  surface of about 8 molecules per  $\text{nm}^2$ , which equals to the hydroxyl density (5 to 15 OH groups per  $\text{nm}^2$ ) on  $\text{TiO}_2$  surfaces [7,8].

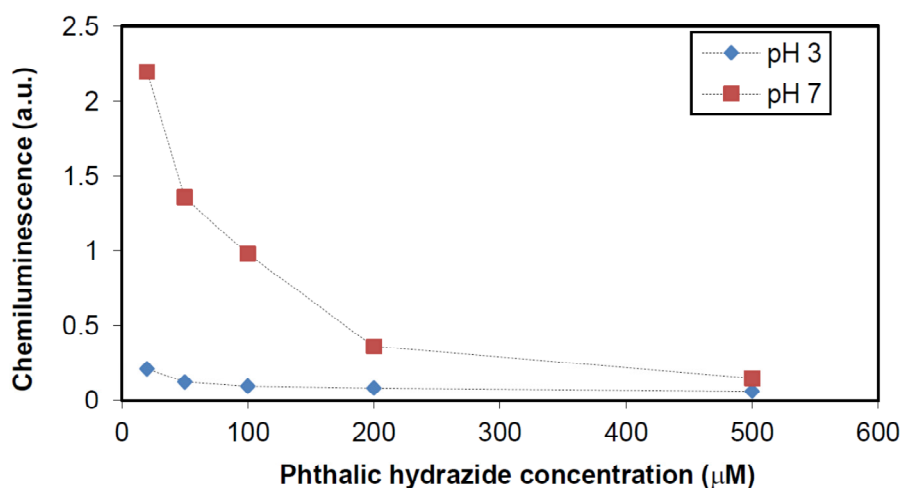
Depending on its thermal history,  $\text{TiO}_2$  preparations contain hydroxyl groups, both terminal and bridged, to varying extent [44]. In presence of water these are involved in acid-based equilibria resulting in a pH-dependent surface charge. At sufficiently low pH the surface is protonated giving a positive charge whereas at high pH the surface is deprotonated leaving the surface negatively charged. At an intermediate pH the surface has zero charge. This is the isoelectric point or the point of zero charge, pzc. For Degussa P25 pzc occurs at pH  $\sim$ 6.3.

Deprotonation of both phthalic hydrazide (pKa = 5.87 [29]) and hydroxyl groups on the  $\text{TiO}_2$  surface occurs at pH > pzc. This creates repulsive conditions and less adsorption is expected. This is clearly seen in Figure 10 and the lack of chemiluminescence signal at pH < 6 seen in Figures 8 and 9 can, partly at least, be ascribed adsorption of phthalic hydrazide on  $\text{TiO}_2$  particles.

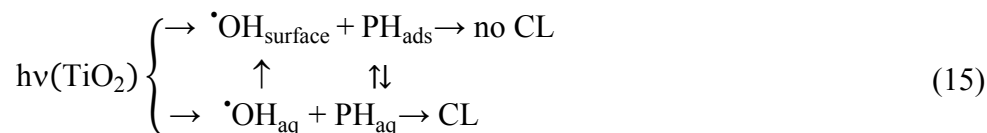
Since phthalic hydrazide can be adsorbed on  $\text{TiO}_2$  surfaces, one may expect a higher chemiluminescence signal when the concentration of phthalic hydrazide is reduced. This was tested in

unbuffered solutions at pH 3, 7 and 9. It was found that at pH 9, the concentration of phthalic hydrazide has only little effect, whereas at pH 7, 50  $\mu\text{M}$  phthalic hydrazide gave rise to about 10 times higher chemiluminescence signal than that obtained by 500  $\mu\text{M}$  phthalic hydrazide. Hence, it looks like adsorption of phthalic hydrazide to  $\text{TiO}_2$  blocks the release of hydroxyl radicals at  $\text{pH} < 9$ , whereas at  $\text{pH} \geq 9$  hydroxyl radicals are able to diffuse from the  $\text{TiO}_2$  surface and can be detected as free species, *i.e.*,  $\cdot\text{OH}_{\text{aq}}$ , through their reactions with phthalic hydrazide. Results for pH 3 and 7 are shown in Figure 11.

**Figure 11.** Effect of phthalic hydrazide concentration on luminescence.



For analysis of the results we assume following competing reactions (PH = phthalic hydrazide):



Under quasi-stationary conditions a solution of this reaction system is:

$$\text{CL} = \frac{\text{CL}_0}{1 + K[\text{PH}]_{\text{ads}}} \quad (16)$$

where  $\text{CL}_0$  is the chemiluminescence obtained when  $[\text{PH}]_{\text{ads}} \rightarrow 0$ , and  $K$  is a collective constant at given reaction conditions.

Suppose the adsorption of phthalic hydrazide (PH) follows a Langmuir isotherm [8,18], then the surface density of phthalic hydrazide,  $[\text{PH}]_{\text{ads}}$ , can be expressed as follows:

$$[\text{PH}]_{\text{ads}} = \frac{\alpha[\text{PH}]_{\text{aq}}}{1 + \alpha[\text{PH}]_{\text{aq}}} [\text{PH}]_{\text{ads}}^* \quad (17)$$

where,  $[\text{PH}]_{\text{aq}}$  is the bulk concentration of phthalic hydrazide,  $\alpha$  is a Langmuir adsorption constant, and  $[\text{PH}]_{\text{ads}}^*$  is the maximum possible phthalic hydrazide surface density on  $\text{TiO}_2$ , and should be a constant. Combining Equation (16) with Equation (17) gives:

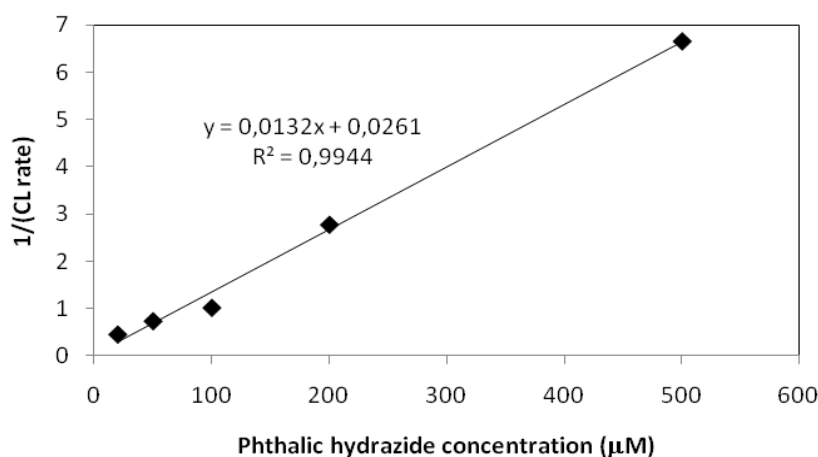
$$CL = \frac{CL_0}{1 + K[PH]_{ads}^* \frac{\alpha[PH]_{aq}}{1 + \alpha[PH]_{aq}}} \quad (18)$$

It is reasonable to assume that the  $[PH]_{ads}$  is far from saturation at  $[PH]_{aq} < 500 \mu\text{M}$ , *i.e.*,  $\alpha[PH]_{aq} \ll 1$ . With this simplification we obtain:

$$\frac{1}{CL} = \frac{1}{CL_0} + \frac{\alpha K [PH]_{ads}^*}{CL_0} [PH]_{aq} \quad (19)$$

The relation of reciprocal chemiluminescence and concentration of phthalic hydrazide is plotted in Figure 12.

**Figure 12.**  $1/CL$  plotted vs. phthalic hydrazide concentration at pH 7.



Evidently, Equation (19) is corroborated by the experimental result. This also lends support to the underlying mechanistic model proposed in Equation (15).

This study clearly demonstrates that adsorption of the reaction probe, in this case phthalic hydrazide, governs the result obtained regarding photocatalytic efficiency of  $\text{TiO}_2$ . Specific for phthalic hydrazide is that this adsorption engages the hydrazide moiety, which can be hydrogen bonded to OH-groups on the surface. Thus, as shown in Figure 2, any surface bound oxidant will only cause oxidation of the hydrazide ring, and no chemiluminescence will be observed. For this reason, we conclude that chemiluminescence can only be observed when  $\cdot\text{OH}_{aq}$  radicals are released from the  $\text{TiO}_2$ -surface.

Another important conclusion from this experiment is that in the unperturbed system at pH  $\sim 7$  free hydroxyl radicals,  $\cdot\text{OH}_{aq}$ , can be released from  $\text{TiO}_2$  at least to the same rate as obtained with borate buffer at pH 9, see Figure 9. In contrast, at pH 3 there is only a vestige of the dilution effect observed at pH  $\sim 7$ . This suggests that increasing protonation of the  $\text{TiO}_2$  surface at pH  $< pzc$  (point of zero charge)  $\approx 6.3$ , also blocks the formation of  $\cdot\text{OH}_{aq}$  whereas at pH  $> pzc$  the measured yield of  $\cdot\text{OH}_{aq}$  is entirely governed by the adsorption of phthalic hydrazide.

### 2.2.2. Effects of Added Hydrogen Peroxide

As shown in Reactions (2–7) addition of hydrogen peroxide may both increase and impair the formation of hydroxyl radicals by TiO<sub>2</sub> photocatalysis in aqueous solutions. The effects should be governed by actual reaction conditions such as pH, ionic composition and the concentration of hydrogen peroxide. Reaction (2) is efficient in the UVC range, where the absorption by hydrogen peroxide is significant [21]. At 365 nm, the peak wavelength of the black light lamp used in this investigation, the absorption of hydrogen peroxide is very weak but Reaction (4) may still give a small contribution to the formation of hydroxyl radicals.

To elucidate some aspects of hydrogen peroxide on the yield of hydroxyl radical formation the experiments in Table 1 were performed (PH = phthalic hydrazide):

**Table 1.** Effects of added hydrogen peroxide.

| Item   | PH  | CL <sub>rate</sub> (a.u.) |
|--|-----|---------------------------|
| A. No pH adjustment, 1 mM H <sub>2</sub> O <sub>2</sub> , 100 ppm TiO <sub>2</sub> , 50 μM PH        | 4.6 | 0.853                     |
| B. No pH adjustment, 1 mM H <sub>2</sub> O <sub>2</sub> , 50 μM PH                                   | 6.1 | 0.255                     |
| C. 1 mM HClO <sub>4</sub> , 1 mM H <sub>2</sub> O <sub>2</sub> , 100 ppm TiO <sub>2</sub> , 50 μM PH | 2.7 | 3.17                      |
| D. 1 mM HClO <sub>4</sub> , 1 mM H <sub>2</sub> O <sub>2</sub> , 50 μM PH                            | 2.7 | 0.324                     |
| E. 1 mM HClO <sub>4</sub> , 100 ppm TiO <sub>2</sub> , 50 μM PH                                      | 2.7 | 0.126                     |

From Table 1 the following conclusions can be drawn:

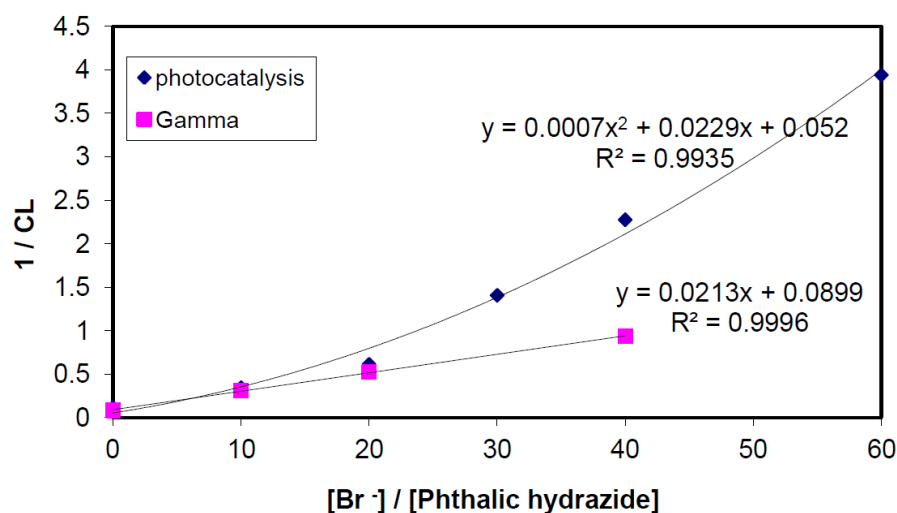
- Comparisons between items E, D and B show that a small yield of <sup>•</sup>OH<sub>aq</sub> can be obtained by photolysis of H<sub>2</sub>O<sub>2</sub> at 365 nm. However, considering the absorbance of 365 nm UV light by TiO<sub>2</sub> (~2.0 at 100 ppm), the contribution from direct photolysis of H<sub>2</sub>O<sub>2</sub> can be neglected in the photocatalytic case;
- Comparisons between items E, C and A show that a significant yield of <sup>•</sup>OH<sub>aq</sub> can be obtained by reductive cleavage of H<sub>2</sub>O<sub>2</sub> at 365 nm;
- Comparisons between items C and A show that of <sup>•</sup>OH<sub>aq</sub> by reductive cleavage of H<sub>2</sub>O<sub>2</sub> at 365 nm depends on pH, and low pH promotes a higher yield. This trend is in accordance with the reaction suggested in Equation (3).

A crucial question is whether hydroxyl radical formation in TiO<sub>2</sub>-photocatalysis can be preferentially assigned to oxidative or reductive reaction pathways. Judging from the pH-behaviour observed with added hydrogen peroxide and taking into consideration that the amount of hydrogen peroxide that may accumulate in the photocatalytic experiments is <0.1 mM, it seems difficult to ascribe the reductive pathway a significant role in the present study. Moreover, it would be difficult to explain how adsorption of phthalic hydrazide on TiO<sub>2</sub> surfaces could completely block the release of <sup>•</sup>OH<sub>aq</sub> radicals, *cf.* Figure 8, if they were formed from hydrogen peroxide by the reductive reaction route. In contrast, the oxidative route involves surface oxidants that can react directly with adsorbed phthalic hydrazide and this would efficiently block the formation of <sup>•</sup>OH<sub>aq</sub> radicals.

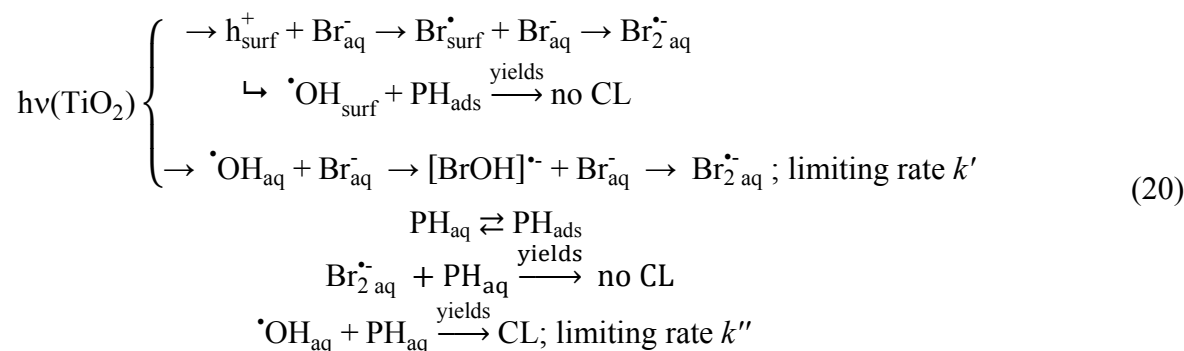
2.2.3. Effects of Br<sup>-</sup> as <sup>•</sup>OH Scavenger

Effects of bromide ions on chemiluminescence in TiO<sub>2</sub>-photocatalysis were studied, at pH 10 in 5 mM borate buffer. In contrast to the simple competition obtained by  $\gamma$ -radiolysis, Figure 6, the plot, Figure 13, indicates a complex multi-step competition.

**Figure 13.** Competition plots obtained by photolysis and  $\gamma$ -radiolysis of 5 mM borate buffer solutions at pH 10 containing NaBr (0–30 mM), phthalic hydrazide (500  $\mu$ M) and 100 ppm TiO<sub>2</sub>.



Because HBr is a very strong acid, bromide ions show no preference to form hydrogen bonds with OH-groups on a TiO<sub>2</sub> surface over linking with water molecules, and no significant adsorption of bromide ions on the TiO<sub>2</sub>-surface is expected to occur. For analysis of the data we assume the following competing reactions:



These reactions translate to:

$$\frac{1}{\text{CL}} = \frac{1}{\text{CL}_0} \left\{ 1 + \frac{k'[\text{Br}^-]_{\text{aq}}}{k''[\text{PH}]_{\text{aq}}} \right\} \left\{ 1 + Q \frac{[\text{Br}^-]_{\text{aq}}}{[\text{PH}]_{\text{aq}}} \right\} \quad (21)$$

where the last term mimics Equation (19)

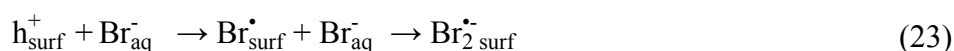
The general form of Equation (21) can be represented as:

$$\frac{1}{CL} = \frac{1}{CL_0} + A \left\{ \frac{[Br^-]_{aq}}{[PH]_{aq}} \right\} + B \left\{ \frac{[Br^-]_{aq}}{[PH]_{aq}} \right\}^2 \quad (22)$$

where A and B are constants.

The curve drawn in Figure 13 is fitted to Equation (22). Apparently, there is a good correspondence between experimental points and Equation (22). For the sake of comparison, the same reaction system was also exposed to  $\gamma$ -radiolysis and the chemiluminescence data were analysed according to the reaction mechanism suggested in Equations (11–13). The initial slopes in the two graphs are very close corroborating our reaction model.

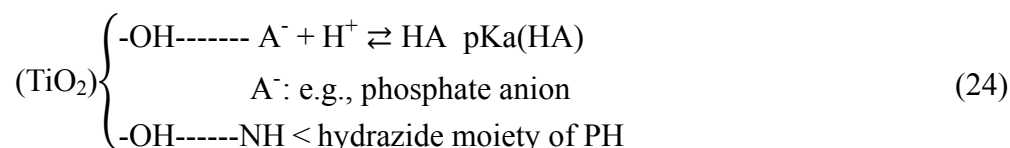
Another aspect related to the suggested reaction model (20), is that formation of dibromidyl radicals,  $Br_2^{\bullet-}$ , on the  $TiO_2$  surface proceeds by:



The first step in Reaction (23) is an outer sphere electron transfer process and it would require that the oxidizing specie formed on the  $TiO_2$  surface, here denoted  $h_{surf}^+$ , is oxidizing enough to allow formation of  $Br_{surf}^{\bullet}$ . Since the reduction potential of  $Br_{aq}^{\bullet}$  is reported to be about 1.9 V vs. NHE [40], the reduction potential of  $h_{surf}^+$  should be at the same level. The reduction potential of  $\equiv Ti[IV]-O^{\bullet}$  sites was assessed to be in the range 1.5–1.7 V vs. NHE [21]. We thus conclude that  $h_{surf}^+$  cannot be ascribed to  $\equiv Ti[IV]-O^{\bullet}$  sites for energetic reasons. Valence band holes ( $h_{VB}^+$ ) reaching the  $TiO_2$  surface can be chemically associated with oxygen-centered radicals generated from surface hydroxyls [7,15], and lattice oxygen anions [10]. Only the latter can then be assigned  $h_{surf}^+$ .

#### 2.2.4. Effects of Added Phosphate and Fluoride Anions

It is known that anions such as phosphate show a strong tendency to be bound on  $TiO_2$  surfaces [45]. When adsorption of phthalic hydrazide to  $TiO_2$  at different pH values was measured in presence of 5 mM phosphate by the spectrophotometric method described in 3.2.1, no significant adsorption could be detected. Thus, addition of phosphate can be used not only to attain pH-buffering but also to control the adsorption of other molecules to a  $TiO_2$  surface. The Reaction (24) is an attempt to explain how this can be. Both phthalic hydrazide, by its hydrazide moiety, and phosphate ions can be linked to OH-groups on the surface by hydrogen bonds. At sufficient high concentration of phosphate there will be no free OH-groups available for phthalic hydrazide and its adsorption to the  $TiO_2$  surface is blocked.



Free hydroxyl radicals do not react with fluoride ions and their reaction rate with phosphate ions ( $HPO_4^{2-}/H_2PO_4^-$ ) is reported to be  $2.0 \times 10^4/M \cdot s$  [46]. Far smaller compared with the above determined reaction rate of hydroxyl radicals with phthalic hydrazide,  $3.4 \times 10^9/M \cdot s$ . Thus, in a solution containing  $5.0 \times 10^{-4}$  M phthalic hydrazide, 0.1 M phosphate can be added before a noticeable scavenging of free hydroxyl radicals by phosphate is reached. However, since phosphate ions are adsorbed at the  $TiO_2$  surface, where hydroxyl radicals occur, the local concentration of phosphate ions

is probably much higher and the scavenging of hydroxyl radicals may become important at considerably lower bulk concentrations than 0.1 M phosphate.

Since addition of phosphate ions can block the adsorption of phthalic hydrazide to  $\text{TiO}_2$  particles increased chemiluminescence can be expected if the phosphate complex on the  $\text{TiO}_2$  surface also allows diffusion of hydroxyl radicals. Recently, additions of fluoride and phosphate ions were also shown to result in increased photocatalytic activities [45,47,48].

The effect of phosphate and fluoride anions on the chemiluminescence yield at pH 3 and 4 is seen in Figure 14.

**Figure 14.** Effect of phosphate and fluoride anions on the chemiluminescence at pH 3 and 4, phthalic hydrazide (500  $\mu\text{M}$ ) and 100 ppm  $\text{TiO}_2$ .

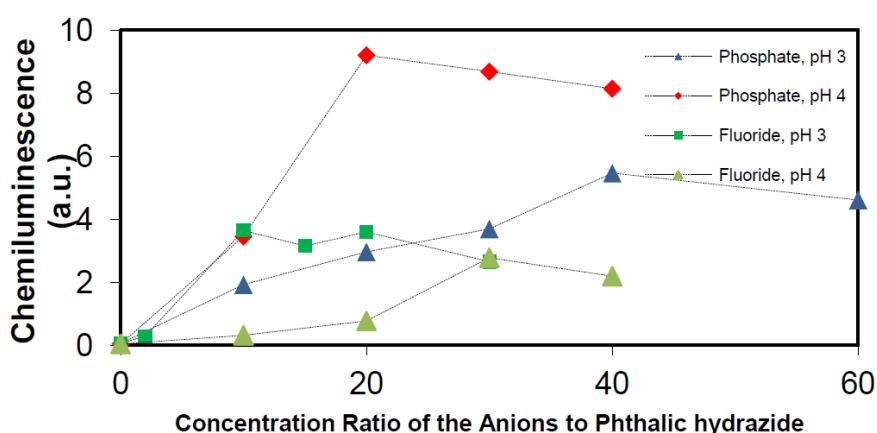


**Figure 15.** Chemiluminescence yield (a.u.) by photocatalysis of  $\text{TiO}_2$  vs. pH. Conditions:  $\text{TiO}_2$  100 ppm; phthalic hydrazide 0.5 mM; 365 nm photon flux  $2.6 \times 10^{-6}$  Einstein/min; water volume 40 mL.

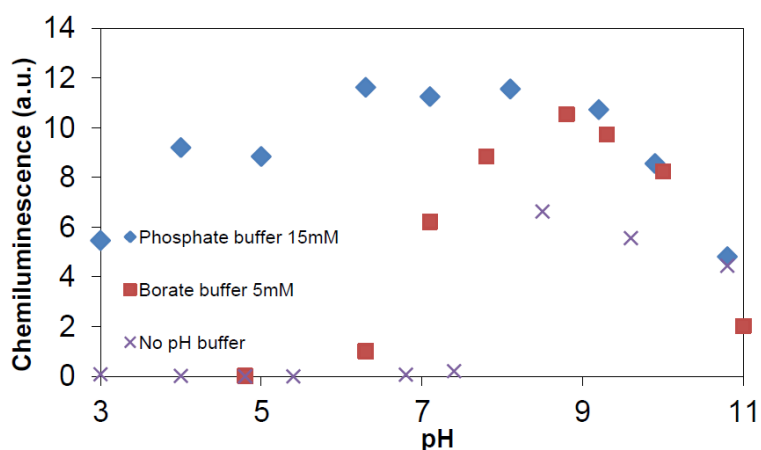


Figure 14 shows that addition of these two ions can substantially increase the chemiluminescence. The enhancement by addition of phosphate ions is higher than that by addition of fluoride ions. When the study was extended, it was found that addition of fluoride ions was only effective at  $\text{pH} < 5$ , ( $\text{pK}_a$  value of HF is about 3.18 [49]), whereas addition of phosphate ions showed an effect in the whole pH-range. Figure 14 also reveals that there is an optimal chemiluminescence yield at a certain concentration of added anions. For the addition of phosphate, this optimum concentration corresponds

to about 15 mM under present conditions. Hence, the full potential of  $\cdot\text{OH}_{\text{aq}}$  radical production in the  $\text{TiO}_2$  photocatalytic system, may be achieved by addition of 15 mM phosphate ions. The resulting chemiluminescence is shown in Figure 15, where also the above already reported results obtained with borate (Figure 9) and no buffer (Figure 8) are included.

Evidently, the chemiluminescence obtained with 15 mM phosphate buffer closely resembles that in Figure 7, where authentic hydroxyl radicals were produced by  $\gamma$ -irradiation at a rate of  $2.7 \mu\text{M}/\text{min}$ . As all chemiluminescence measurements have been performed in a standardized manner, we can now assess the hydroxyl radical production rate in photocatalysis from:

$$(\cdot\text{OH}_{\text{aq}}\text{-radical production rate})_{\lambda} = 2.7 \mu\text{M}/\text{min} \frac{\text{CL}(\text{Figure 15})}{\text{CL}(\text{Figure 7})} \quad (25)$$

The result of this calibration is shown in Figure 16.

**Figure 16.** Production rate of  $\cdot\text{OH}_{\text{aq}}$ -radicals by  $\text{TiO}_2$  photocatalysis vs. pH. Conditions:  $\text{TiO}_2$  100 ppm; phthalic hydrazide 0.5 mM; phosphate buffer 15 mM; 365 nm photon flux  $2.6 \times 10^{-6}$  Einstein/min; water volume 40 mL.

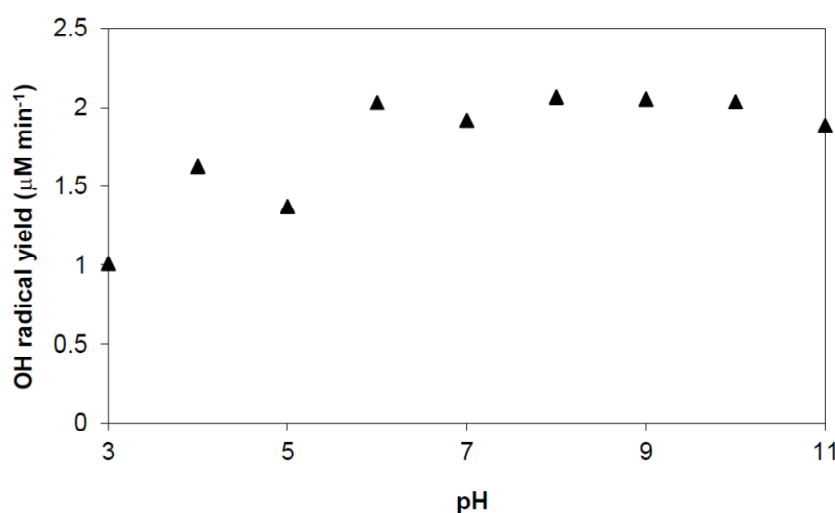


Figure 16 shows a nearly constant  $\cdot\text{OH}_{\text{aq}}$  radical production rate in the studied pH range with a slight decreasing at  $\text{pH} < \text{pzc}$ . The top  $\cdot\text{OH}_{\text{aq}}$  radical yield is  $\sim 2.1 \mu\text{M}/\text{min}$ , which would correspond to an “apparent quantum efficiency” of about 3.2% (Determination of quantum efficiency is not straightforward. The problem comes in measuring the optical absorption efficiency of a particular  $\text{TiO}_2$  sample because of complications associated with light scattering and penetration. Often the ratio of detected events per incident photon is reported as “apparent quantum efficiency”. However, what one would like to know is the ratio of detected events per incident *absorbed* photon. Comparisons of “apparent quantum efficiencies” are only meaningful if effects due to light scattering and penetration are comparable.) The pH trend and the “apparent quantum efficiency” obtained in this study is similar to what has been reported in previously published works [50,51], where methanol was used as general OH radical probe with a very low tendency to be adsorbed on  $\text{TiO}_2$  surfaces. However, our “apparent quantum efficiency” is at variance with the much smaller value reported by Hirakawa *et al.* [26]. These authors have used a generically similar method to ours, *i.e.*, it is based on transformation of an original molecule by aromatic hydroxylation into a hydroxylated analogue that can be detected by emission of

photons. In their case detection is by fluorescence and the original molecule is terephthalic acid (TPA). Both methods are selective and very sensitive. Compared with our chemiluminescence method the TPA fluorescence method is probably more easily adapted and may also allow continuous measurement. However, in the cited work by Hirakawa *et al.* [26], the method has been applied beyond its perimeters. At the chosen wavelength 385 nm, the extinction of Degussa P25 TiO<sub>2</sub> suspensions is almost entirely due to scattering, absorption is virtually zero [52]. The chosen pH, pH ~12, is also too high. At this pH, hydroxyl radicals are to a large extent deprotonated (pK<sub>a</sub> <sup>•</sup>OH = 11.9 at 25 °C [53]). The anionic form, the oxyl radical anion, O<sup>•-</sup> displays properties distinctly different from those of the hydroxyl radical; nucleophilic addition, hydrogen atom abstraction but no tendency to add to aromatic rings [53]. It is a very reactive radical and will attack TPA, e.g., by nucleophilic elimination of carboxylic groups. Only electrophilic <sup>•</sup>OH<sub>aq</sub> radicals can amalgamate with π-electrons in an aromatic ring to form cyclohexadienyl adducts that after oxidation result in aromatic ring hydroxylation products. In the TPA system this oxidation is very slow with molecular oxygen due to the reversible addition of oxygen to a TPA-hydroxycyclohexadienyl adduct [54]. This allows a range of alternative reaction pathways, particularly at high pH, and significant reduction in formation of fluorescent 2-OH-TPA.

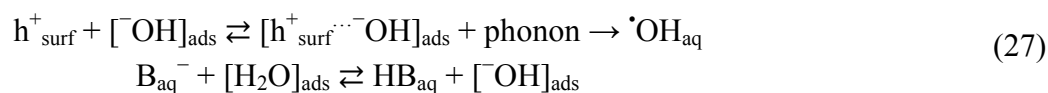
#### 2.2.5. Formation of <sup>•</sup>OH<sub>aq</sub> Radicals

We have already concluded that <sup>•</sup>OH<sub>aq</sub> radicals under prevailing conditions must arise predominantly by the oxidative route, *i.e.*, by transformations originating in the formation of valence band holes (h<sub>VB</sub><sup>+</sup>). However, albeit that from thermodynamic point of view these sites can oxidize water to produce <sup>•</sup>OH<sub>aq</sub>, Salvador [20] has calculated that the highest energy levels of adsorbed water species on TiO<sub>2</sub> are well below the valence band edge of TiO<sub>2</sub>. This would thus exclude that <sup>•</sup>OH<sub>aq</sub> can be formed by the oxidative route as we have found. A possible solution of this dilemma is offered by a Cheng and Selloni [55] who have done extensive first principles molecular dynamics simulations for a hydrated hydroxide ion on a TiO<sub>2</sub> anatase (101) surface. They found that, due to thermal fluctuations, hydroxyl ion energy levels can occur above the valence band edge of anatase TiO<sub>2</sub> and thus allow formation of <sup>•</sup>OH<sub>aq</sub> radicals. We interpret their result as:



where [OH]<sub>ads</sub> is an OH<sup>-</sup> ion in the water layer associated with the TiO<sub>2</sub> surface, and [h<sub>surf</sub><sup>+</sup>⋯OH]<sub>ads</sub> is a charge transfer complex at the TiO<sub>2</sub> surface.

As demonstrated in Figure 10, the unperturbed system at pH ~7 can release free hydroxyl radicals, <sup>•</sup>OH<sub>aq</sub>, from TiO<sub>2</sub> at least to the same rate as obtained by addition of 15 mM phosphate buffer. This implies that at pH ≥ pzc (≈6) oxidation stable bases, such as H<sub>2</sub>PO<sub>4</sub><sup>-</sup>, HPO<sub>4</sub><sup>2-</sup>, and HB<sub>4</sub>O<sub>7</sub><sup>-</sup>, adsorbed on the TiO<sub>2</sub> surface, enhances the measured yield of <sup>•</sup>OH<sub>aq</sub> merely by blocking the adsorption of phthalic hydrazide, but they are not directly involved in the formation of <sup>•</sup>OH<sub>aq</sub>. At pH ≤ pzc, oxidation stable bases, such as H<sub>2</sub>PO<sub>4</sub><sup>-</sup> and F<sup>-</sup>, may also be involved in the formation of <sup>•</sup>OH<sub>aq</sub> by “neutralizing” protons on the TiO<sub>2</sub> surface and enhancing the presence of hydroxide ions in the water layer associated with the TiO<sub>2</sub> surface. Combined with Equation (26) we thus suggest that formation of <sup>•</sup>OH<sub>aq</sub> by the oxidative route can be summarized by the mechanism:



where  $\text{B}^-$  is an oxidation stable base, e.g.,  $\text{H}_2\text{PO}_4^-$  and  $\text{F}^-$ .

### 3. Experimental Section

#### 3.1. Materials and Preparations

All chemicals used were of analytical grade or higher and used as received from commercial sources (Sigma-Aldrich Sweden AB, Degussa, Germany). Millipore Mill-Q filtered water was used in all experiments.  $\text{TiO}_2$  powder used in this study was Degussa P25 with a reported average primary particle size of 21 nm and a specific surface area of  $50 \pm 15 \text{ m}^2/\text{g}$  (BET) according to the manufacturer. However, the actual diameter of formed aggregates in Millipore water was found to be about 500 nm when measured by a Brookhaven 90 Plus laser scattering particle size analyzer.

Phthalic hydrazide (2,3-dihydro-1,4-phthalazinedione) is a weak acid ( $\text{p}K_{\text{a}1} = 5.87$  and  $\text{p}K_{\text{a}2} = 14.75$  [29]). At room temperature and at near neutral pH the solubility is about 0.6 mM. In most experiments, the concentration of phthalic hydrazide was 0.5 mM. 3-Hydroxyphthalic hydrazide (2,3-dihydro-5-hydroxy-1,4-phthalazinedione) was synthesized as described by Drew and Pearman [37].

pH was adjusted either directly by NaOH and  $\text{HClO}_4$  or by phosphate or borate pH buffers. The actual pH value was measured with a Metrohm 713 pH meter, calibrated against standard buffers.

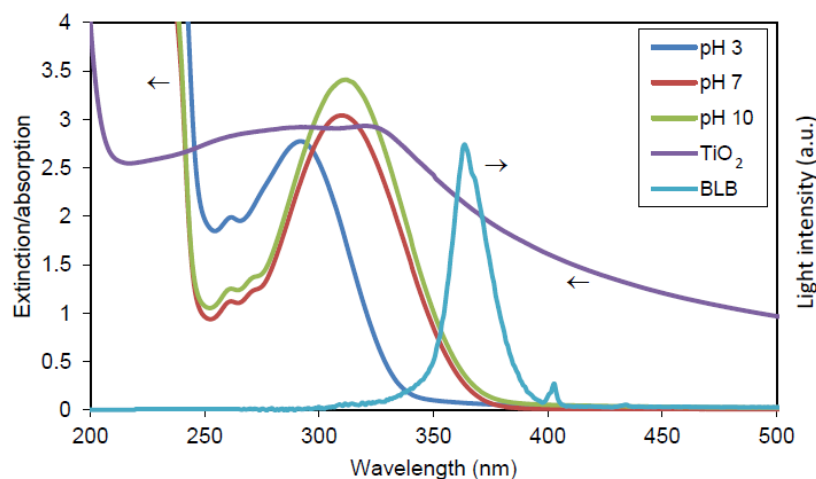
#### 3.2. Irradiations

*Gamma irradiations* were carried out in a Cesium-137 source (Gammacell 1000 Elite, Best Theratronics, Ottawa, Canada). All irradiations were performed in the same vessel containing 40 mL solution. The dose rate in this volume was determined by Fricke dosimetry [12] to be 9.5 Gy/min. This translates to an OH-radical production rate of 2.70  $\mu\text{M}/\text{min}$  [12]

*Photocatalytic experiments* were performed under two Blacklight blue, BLB, lamps (Philips TL-D 15 W, Philips AB Stockholm, Sweden). Spectrum of this type of BLB lamp, extinction spectrum of 100 ppm Degussa  $\text{TiO}_2$ , and absorption spectra of 500  $\mu\text{M}$  phthalic hydrazide at different pH values are shown in the figure below, Figure 17.

The wavelength range and peak wavelength were determined (Hamamatsu PMA-12 spectrometer) to be 345–385 and 365 nm, respectively, with an average intensity of 0.2  $\text{mW}/\text{cm}^2$  at the irradiation distance (International Light ILT1400 radiometer). All samples to be irradiated were placed in a blackened Petri dish (glass) of 9.5 cm inner diameter. The irradiated volume was 40 mL. The samples were stirred by a magnetic Teflon coated stirrer to obtain a homogenous mixing of the  $\text{TiO}_2$  suspension. The absorbed 365 nm photon flux is thus  $6.5 \times 10^{-5}$  Einstein/L·min in the irradiated volume based on the average photon intensity.

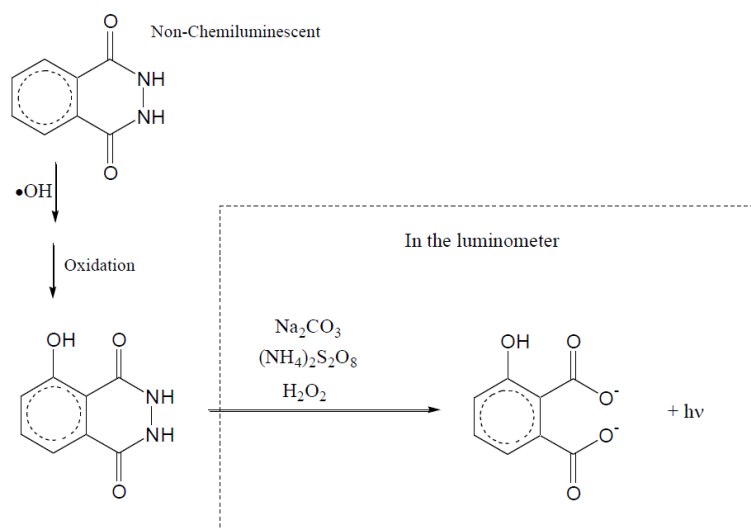
**Figure 17.** Extinction spectrum of 100 ppm Degussa TiO<sub>2</sub>, absorption spectra of 500 μM phthalic hydrazide in Millipore water at pH 3,7,10, and the radiation spectrum of black light blue lamp (BLB).



### 3.3. Chemiluminescence Measurements

Figure 18 presents the chemiluminescence measurement process. At appropriate time intervals a sample (about 2 mL) of the reaction mixture was withdrawn with a syringe and filtered through a 0.2 μm membrane filter (Whatman OE 66, Sigma-Aldrich, Stockholm, Sweden). One hundred microliters of the filtered solution was mixed with 1 mL 1M Na<sub>2</sub>CO<sub>3</sub> containing 1 mM diethylene triamine pentaacetic acid (DTPA), 100 μL 0.1 M (NH<sub>4</sub>)<sub>2</sub>S<sub>2</sub>O<sub>8</sub> and 100 μL 0.1 M H<sub>2</sub>O<sub>2</sub> in an optical cuvette. The cuvette was agitated for about one minute in a shaking apparatus and then transferred to a luminometer (Biorbit, 1250 with PC interface and software), and the CL signal was measured.

**Figure 18.** Chemiluminescence method to detect the formation of hydroxyl radicals. A small amount of phthalic hydrazide is added to the reaction system. At selected intervals, samples are removed from the reaction liquor for analysis in a luminometer.



Using this procedure, phthalic hydrazides are slowly oxidized by persulfate to the corresponding azaquinones, which are nucleophilically attacked by peroxide anions [56]. The chemiluminescence obtained in this way is fairly stable for several minutes and the signal is read as the height of the trace above the background level. A low background is obtained when the development of the chemiluminescence is performed in 1 M Na<sub>2</sub>CO<sub>3</sub> solutions containing a complexing agent such as DTPA [28,29]. A high concentration of carbonate offers pH-buffer capacity, and scavenging of adventitious hydroxyl radicals that may arise in the mixing of the reagents:



The carbonate radical is a one-electron oxidant [40] that will only oxidize the hydrazide moiety to the corresponding phthalic acid.

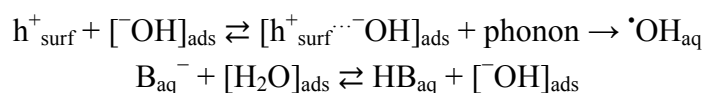
All studies were performed in temporal stages and the linear increase in chemiluminescence was measured as  $\frac{\Delta\text{CL}}{\Delta t} = \text{a.u.}$ . The total conversion of added phthalic hydrazide was controlled to be no more than 10%.

#### 4. Conclusions

This work demonstrates how formation of strongly chemiluminescent 3-hydroxyphthalic hydrazide by hydroxylation of non-chemiluminescent phthalic hydrazide can be applied as a selective reaction probe to obtain information on authentic hydroxyl radical, *i.e.*,  $\cdot\text{OH}_{\text{aq}}$ , formation, in black light illuminated Degussa P25 TiO<sub>2</sub> aerated suspensions.

At pH  $\geq$  pzc (~6.3), it was found that oxidation stable bases, such as H<sub>2</sub>PO<sub>4</sub><sup>-</sup>, HPO<sub>4</sub><sup>2-</sup>, and HB<sub>4</sub>O<sub>7</sub><sup>-</sup>, adsorbed on the TiO<sub>2</sub> surface, enhances the measured yield of  $\cdot\text{OH}_{\text{aq}}$  merely by blocking the adsorption of phthalic hydrazide, but they are not directly involved in the formation of  $\cdot\text{OH}_{\text{aq}}$ . At pH  $\leq$  pzc, oxidation stable bases, such as H<sub>2</sub>PO<sub>4</sub><sup>-</sup> and F<sup>-</sup>, adsorbed on the TiO<sub>2</sub> surface may also be involved in the formation of  $\cdot\text{OH}_{\text{aq}}$  by enhancing the presence of hydroxide ions at the TiO<sub>2</sub> surface. Under most optimized conditions in our experimental tests (addition of optimized concentration of appropriate oxidation stable bases), the  $\cdot\text{OH}_{\text{aq}}$  radical production rate in the pH range 7–11 was nearly constant (“apparent quantum efficiency” ~3.2% under prevailing conditions) but decreased slightly at pH < pzc.

We suggest that the formation of  $\cdot\text{OH}_{\text{aq}}$  by the oxidative route can be summarized by the mechanism:



where  $[\text{}^-\text{OH}]_{\text{ads}}$  is an  $\text{}^-\text{OH}$  ion in the water layer associated with the TiO<sub>2</sub> surface,  $[h^+_{\text{surf}} \cdots \text{}^-\text{OH}]_{\text{ads}}$  is a charge transfer complex at the TiO<sub>2</sub> surface, and B<sup>-</sup> is an oxidation stable base, e.g., H<sub>2</sub>PO<sub>4</sub><sup>-</sup> and F<sup>-</sup>.

#### Acknowledgments

Financial support from Wallenius Water AB, Stockholm is gratefully acknowledged. We are also indebted to our reviewers for valuable suggestions.

## Conflict of Interest

The authors declare no conflict of interest.

## References

1. Ohtani, B. Photocatalysis A to Z - What we know and what we do not know in a scientific sense. *J. Photochem. Photobiol. C* **2010**, *11*, 157–178.
2. Keshmiri, M.; Mohseni, M.; Troczynski, T. Development of a novel TiO<sub>2</sub> sol-gel derived composite and its photocatalytic activities for trichloroethylene oxidation. *Appl. Catal. B* **2004**, *53*, 209–219.
3. Agustina, T.E.; Ang, H.M.; Vareek, V.K. A review of synergistic effect of photocatalysis and ozonation of wastewater treatment. *J. Photochem. Photobiol. C* **2005**, *6*, 264–273.
4. Malato, S.; Blanco, J.; Alarcon, D.C. Photocatalytic decontamination and disinfection of water with solar collectors. *Catal. Today* **2007**, *122*, 137–149.
5. Mukherjee, P.S.; Ray, A.K. Major challenges in the design of a large-scale photocatalytic reactor for water treatment. *Chem. Eng. Technol.* **1999**, *22*, 253–260.
6. Choo, K.H.; Tao, R.; Kim, M.J. Use of a photocatalytic membrane reactor for the removal of natural organic matter in water. Effect of photoinduced desorption and ferrihydrite adsorption. *J. Membr. Sci.* **2008**, *322*, 368–374.
7. Hurum, D.C.; Agrios, A.G.; Gray, K.A.; Rajh, T.; Thurnauer, M.C. Explaining the enhanced photocatalytic activity of Degussa P25 mixed-phase TiO<sub>2</sub> using EPR. *J. Phys. Chem. B* **2003**, *107*, 4545–4549.
8. Turchi, C.S.; Ollis, D.F. Photocatalytic degradation of organic water contaminants; mechanisms involving hydroxyl radical attack. *J. Catal.* **1990**, *122*, 178–192.
9. Fujishima, A.; Zhang, X.T.; Tryk, D.A. TiO<sub>2</sub> photocatalysis and related surface phenomena. *Surf. Sci. Rep.* **2008**, *63*, 515–582.
10. Howe, R.F.; Grätzel, M. EPR observation of trapped electrons in colloidal titanium dioxide. *J. Phys. Chem.* **1985**, *89*, 4495–4499.
11. Dung, D.; Ramsden, J.; Graetzel, M. Dynamics of interfacial electron-transfer processes in colloidal semiconductor systems. *J. Am. Chem. Soc.* **1982**, *104*, 2977–2985.
12. Spinks, J.W.T.; Woods, R.J. *An Introduction to Radiation Chemistry*, 3rd ed.; John Wiley and Sons Inc: New York, NY, USA, 1990.
13. Lee, J.; Park, H.; Choi, W. Selective photocatalytic oxidation of NH<sub>3</sub> to N<sub>2</sub> on platinumized TiO<sub>2</sub> in water. *Environ. Sci. Technol.* **2002**, *36*, 5462–5468.
14. Nakamura, R.; Imanishi, A.; Murakoshi, K.; Nakato, Y. *In situ* FTIR studies of primary intermediates of photocatalytic reactions on nanocrystalline TiO<sub>2</sub> films in contact with aqueous solutions. *J. Am. Chem. Soc.* **2003**, *125*, 7443–7450.
15. Micic, O.I.; Zhang, Y.; Cromack, K.R.; Trifunac, A.D.; Thurnauer, M.C. Trapped holes on titania colloids studied by electron paramagnetic resonance. *J. Phys. Chem.* **1993**, *97*, 7277–7283.
16. Murakami, Y.; Endo, K.; Ohta, I.; Nosaka, A.Y.; Nosaka, Y. Can OH radicals diffuse from the UV-irradiated photocatalytic TiO<sub>2</sub> surfaces? Laser-induced fluorescence study. *J. Phys. Chem. C* **2007**, *111*, 11339–11346.

17. Mills, A.; Hunte, S.L. An overview of semiconductor photocatalysis. *J. Photochem. Photobiol. A* **1997**, *108*, 1–35.
18. Ishibashi, K.; Fujishima, A.; Watanabe, T.; Hashimoto, K. Quantum yields of active oxidative species formed on TiO<sub>2</sub> photocatalyst. *J. Photochem. Photobiol. A* **2000**, *134*, 139–142.
19. Goldstein, S.; Czapski, G.; Rabani, J. Oxidation of phenol by radiolytically generated <sup>•</sup>OH and Chemically Generated SO<sub>4</sub><sup>•-</sup>. A Distinction between <sup>•</sup>OH transfer and hole oxidation in in the photolysis of TiO<sub>2</sub> colloid solution. *J. Phys. Chem.* **1994**, *98*, 6586–6591.
20. Salvador, P. On the nature of photogenerated radical species active in the oxidative degradation of dissolved pollutants with TiO<sub>2</sub> aqueous suspensions: A revision in the light of the electronic structure of adsorbed water. *J. Phys. Chem. C* **2007**, *111*, 17038–17043.
21. Lawless, D.; Serpone, N.; Meisel, D. Role of hydroxyl radicals and trapped holes in photocatalysis. A pulse radiolysis study. *J. Phys. Chem.* **1991**, *95*, 5166–5170.
22. Oppenländer, T. *Photochemical Purification of Water and Air*; WILEY-VCH Verlag GmbH & Co.: Weinheim, Germany, 2003.
23. Sun, L.; Bolton, J.R. Determination of the quantum yield for the photochemical generation of hydroxyl radicals. *J. Phys. Chem.* **1996**, *100*, 4127–4134.
24. Diesen, V.; Jonsson, M.J. Tris(hydroxymethyl) aminomethane as a probe in heterogeneous TiO<sub>2</sub> photocatalysis. *Adv. Oxid. Technol.* **2012**, *15*, 392–398.
25. Ishibashi, K.; Fujishima, A.; Watanabe, T.; Hashimoto, K. Detection of active oxidative species in TiO<sub>2</sub> photocatalysis using the fluorescence technique. *Electrochem. Commun.* **2000**, *2*, 207–210.
26. Hirakawa, T.; Nosaka, Y. Properties of O<sub>2</sub><sup>•-</sup> and OH<sup>•</sup> formed in TiO<sub>2</sub> aqueous suspensions by photocatalytic reaction and the influence of H<sub>2</sub>O<sub>2</sub> and Some Ions. *Langmuir* **2002**, *18*, 3247–3254.
27. Nosaka, Y.; Komori, S.; Yawata, K.; Hirakawa, T.; Nosaka, A.Y. Photocatalytic OH Radical Formation in TiO<sub>2</sub> aqueous suspension studied by several detection methods. *Phys. Chem. Chem. Phys.* **2003**, *5*, 4731–4735.
28. Reitberger, T.; Gierer, J. Chemiluminescence as a means to study the role of hydroxyl radicals in oxidative processes. *Holzforschung* **1988**, *42*, 351–356.
29. Backa, S.; Jansbo, K.; Reitberger, T. Detection of hydroxyl radicals by a chemiluminescence method—A critical review. *Holzforschung* **1997**, *51*, 557–564.
30. Gierer, J.; Jansbo, K.; Reitberger, T. Formation of hydroxyl radicals from hydrogen peroxide and their effect on bleaching of mechanical pulps. *J. Wood Chem. Tech.* **1993**, *13*, 561–581.
31. Backa, S.; Brolin, A. Determination of pulp characteristics by diffuse reflectance FTIR. *Tappi J.* **1991**, *74*, 218–226.
32. Backa, S.; Gierer, J.; Reitberger, T.; Nilsson, T. Hydroxyl radical activity associated with the growth of white-rot fungi. *Holzforschung* **1993**, *47*, 181–187.
33. Miller, C.J.; Rose, A.L.; Waite, T.D. Phthalhydrazide chemiluminescence method for determination of hydroxyl radical production: Modifications and adaptations for use in natural systems. *Anal. Chem.* **2011**, *83*, 261–268.
34. Fang, X.; Pan, X.; Rahmann, A.; Schuchmann, H.-P.; von Sonntag, A.C. Reversibility in the reaction of cyclohexadienyl radicals with oxygen in aqueous solution. *Chem. Eur. J.* **1995**, *1*, 423–429.

35. Bielski, B.H.J.; Cabelli, D.E.; Arudi, R.L.; Ross, A.B. Reactivity of  $\text{HO}_2/\text{O}_2^-$  radicals in aqueous solution. *J. Phys. Chem. Ref. Data* **1985**, *14*, 1041–1100.
36. Jonsson, M.; Lind, J.; Reitberger, T.; Eriksen, T.E.; Merényi, G. Free radical combination reactions involving phenoxyl radicals. *J. Phys. Chem.* **1993**, *97*, 8229–8233.
37. Drew, C.H.D.K.; Pearman, F.H. Chemiluminescent organic compounds. Part II the effect of substituents on the closure of phthalhydrazides to 5- and 6-membered rings. *J. Chem. Soc.* **1937**, *64*, 26–33.
38. Schlosser, D.; Fahr, K.; Karl, W.; Wetzstein, H.-G. Hydroxylated metabolites of 2,4-dichlorophenol imply fenton-type reaction in *Gloeophyllum striatum*. *Appl. Environ. Microbiol.* **2000**, *66*, 2479–2483.
39. Lide, D.R.; Frederiksen, H.P.R. *CRC Handbook of Chemistry and Physics*, 76th ed.; CRC Press Inc.: Boca Raton, FL, USA, 1995.
40. Wardman, P. Reduction potentials of one-electron couples involving free radicals in aqueous solution. *J. Phys. Chem. Ref. Data* **1989**, *18*, 1637–1755.
41. Matheson, M.S.; Mulac, W.A.; Weeks, J.L.; Rabani, J. The pulse radiolysis of deaerated aqueous bromide solutions. *J. Phys. Chem.* **1966**, *70*, 2092–2099.
42. Schiller, J.; Arnhold, J.; Schwinn, J.; Sprinz, H.; Brede, O.; Arnold, K. Differences in the reactivity of phthalic hydrazide and luminol with hydroxyl radicals. *Free Radic. Res.* **1999**, *30*, 45–57.
43. Shultz, A.N.; Hetherington, W.M., III; Baer, D.R.; Wang, L.Q.; Engelhard, M.H. Comparative SHG and XPS studies of interactions between defects and  $\text{N}_2\text{O}$  on rutile (110) surfaces. *Surf. Sci.* **1997**, *392*, 1–7.
44. Connor, P.A.; Dobson, K.D.; McQuillan, A.J. Infrared spectroscopy of the  $\text{TiO}_2$ /aqueous solution interface. *Langmuir* **1999**, *15*, 2402–2408.
45. Zhao, D.; Chen, C.; Wang, Y.; Ji, H.; Ma, W.; Zang, L.; Zhao, J. Surface modification of  $\text{TiO}_2$  by phosphate: Effect on photocatalytic activity and mechanism implication. *J. Phys. Chem. C* **2008**, *112*, 5993–5600.
46. Maruthamuthu, P.; Neta, P. Phosphate radicals, spectra, acid-base equilibria, and reactions with inorganic compounds. *J. Phys. Chem.* **1978**, *82*, 710–713.
47. Brusa, M.A.; Grela, M.A. Experimental upper bound on phosphate radical production in  $\text{TiO}_2$  photocatalytic transformations in the presence of phosphate ions. *Phys. Chem. Chem. Phys.* **2003**, *5*, 3294–3298.
48. Xu, Y.; Lv, K.; Xiong, Z.; Leng, W.; Du, W.; Liu, D.; Xue, X. Rate enhancement and rate inhibition of phenol degradation over irradiated anatase and rutile  $\text{TiO}_2$  on the addition of NaF: New insight into the mechanism. *J. Phys. Chem. C* **2007**, *111*, 19024–19032.
49. Petrucci, R.H.; Harwood, W.S.; Herring, F.G. *General Chemistry*, 8th ed.; Pearson Prentice Hall, Pearson Education Inc.: Upper Saddle River, NJ, USA, 2002; p. 678.
50. Du, Y.; Rabani, J. The measure of  $\text{TiO}_2$  photocatalytic efficiency and the comparison of different photocatalytic titania. *J. Phys. Chem. B* **2003**, *107*, 11970–11978.
51. Wang, C.; Rabani, J.; Bahnemann, D.W.; Dohrmann, J.K. Photonic efficiency and the quantum yield of formaldehyde from methanol in the presence of various  $\text{TiO}_2$  photocatalysts. *J. Photochem. Photobiol. A* **2002**, *148*, 169–176.

52. Cabrera, B.M.I.; Alfano, O.M.; Cassano, A.E. Absorption and scattering coefficients of titanium dioxide particulate suspensions in water. *J. Phys. Chem.* **1996**, *100*, 20043–20050.
53. Buxton, G.V.; Greenstock, C.L.; Helman, W.P.; Ross, A.B. Critical review of rate constants for reactions of hydrated electrons, hydrogen atoms and hydroxyl radicals ( $\cdot\text{OH}/\text{O}^-$ ) in Aqueous solution. *J. Phys. Chem. Data* **1988**, *17*, 513–886.
54. Fang, X.; Mark, G.; von Sonntag, C. OH radical formation by ultrasound in aqueous solutions part I: The Chemistry underlying the terephthale dosimeter. *Ultrason. Sonochem.* **1996**, *3*, 57–63.
55. Cheng, H.; Selloni, A. Hydroxide ions at the water/anatase  $\text{TiO}_2$  (101) interface: Structure and electronic states from first principles molecular dynamics. *Langmuir* **2010**, *26*, 11518–11525.
56. Merenyi, G.; Lind, J.; Eriksen, T.E. Nucleophilic addition to diazaquines, formation and breakdown of tetrahedral intermediates in relation to luminol chemiluminescence. *J. Am. Chem. Soc.* **1986**, *108*, 7716–7726.

© 2013 by the authors; licensee MDPI, Basel, Switzerland. This article is an open access article distributed under the terms and conditions of the Creative Commons Attribution license (<http://creativecommons.org/licenses/by/3.0/>).